Critical Reviews™ in Biomedical Engineering, 39(1):45–62 (2011)

In Vitro Microelectrode Array Technology and Neural Recordings

Yoonkey Nam[1*] *& Bruce C. Wheeler*[2]

[1]Department of Bio and Brain Engineering, KAIST, Republic of Korea; [2]J. Crayton Pruitt Family Department of Biomedical Engineering, University of Florida at Gainesville, Gainesville, FL

*Address all correspondence to Yoonkey Nam, 335 Gwahangno, Yuseong-Gu, Daejeon 305-701, Korea; Tel.: +82-42-350-4322; Fax: +82-42-350-4310; ynam@kaist.ac.kr.

ABSTRACT: In vitro microelectrode array (MEA) technology has evolved into a widely used and effective methodology to study cultured neural networks. An MEA forms a unique electrical interface with the cultured neurons in that neurons are directly grown on top of the electrode (neuron-on-electrode configuration). Theoretical models and experimental results suggest that physical configuration and biological environments of the cell-electrode interface play a key role in the outcome of neural recordings, such as yield of recordings, signal shape, and signal-to-noise ratio. Recent interdisciplinary approaches have shown that MEA performance can be enhanced through novel nanomaterials, structures, surface chemistry, and biotechnology. In vitro and in vivo neural interfaces share some common factors, and in vitro neural interface issues can be extended to solve in vivo neural interface problems of brain-machine interface or neuromodulation techniques.

KEY WORDS: MEA technology, cell-electrode coupling, neural recording, neural interface, microelectrode array

I. INTRODUCTION

Cultured neuronal networks have been used as in vitro model systems in many fields of neuroscience, including synaptogenesis,[1] axon guidance,[2] nerve regeneration,[3] and neural plasticity.[4,5] In addition, special methodologies such as compartmental chambers,[6] micro-island cultures,[7] cell patterning,[8] and organotypic slice culture[9] have been developed for the investigation of the mechanism of neural information processing in neural networks.

In vitro microelectrode array (MEA) technology has been developed to characterize cultured neuronal networks.[10–12] Neurons are cultured on a planar type microelectrode array that is capable of sensing electrical signals from neurons or neural circuits. MEAs are created using microfabrication processes originally developed in the semiconductor industry. By interfacing microelectrodes with individual neurons and measuring extracellular action potentials (spikes), MEAs provide spatiotemporal information of the network activity that can be utilized for the quantitative study of cultured neuronal networks.[13–16]

The quality of the neural recordings is one of the most important factors that determines the success of each experiment as well as the MEA technology overall. Success follows when the networks of neurons are biologically active and the sensors are effective at measuring the bioelectric signals. In this article, neural signal recordings will be reviewed in terms of cell-electrode interfaces and in vitro neural interface design.

ABBREVIATIONS

MEA, microelectrode array; FET, field-effect transistor; DRG, dorsal root ganglion; CNT, carbon nanotube; SAM, self-assembled monolayer; 3GPS, [3-glycidoxypropyl] trimethoxysilane; SNR, signal-to-noise ratio; 11-MUA, 11-mercaptoundecanoic acid; 3APS, 3-amonipropyltrimethoxysilane; PDMS, polydimethoxysiloxane

0278-940X/11/$35.00

II. NEURAL SIGNALS FROM MEA INTERFACES

II.A. Planar-Type Microelectrode Array System

A planar-type MEA is a cell culture dish with an array of embedded surface microelectrodes (Fig. 1[a]). Substrates are usually made of glass wafers so that the observation of live cells can be performed with conventional transmitted light microscopy. Microelectrodes are made of nontoxic, corrosion-resistant metals (e.g., platinum, gold, iridium, titanium nitride); electrodes are insulated from each other and the culture medium using inorganic or organic materials (silicon oxide, silicon nitride, polyimide, epoxy resin). The size of the electrode is in the range of a few tens of micrometers in diameter, which is comparable to the size of single neurons. Each electrode is connected with a contact pad through a thin conductor line so that an extracellular recording amplifier can amplify the signal picked up by the electrode. Since there are multiple electrodes, instrumentation systems are also equipped with multichannel analog and digital signal processors. A 60-electrode MEA is common, and high-density MEAs such as 519-electrode MEAs[17] or light-addressable MEAs with 3600 electrodes[18] have also been reported. For ultra-high-density MEAs, active-pixel-type arrays have been developed. MEA systems with 11,011 electrodes[19], 4096 electrodes,[20] and 128 × 128 electrodes[21] have been successfully tested with cultured neurons.

The number of commercial vendors that fabricate MEAs and instrumentation systems has grown steadily in the last decade, including MultiChannel Systems (Reutlingen, Germany), Alpha MED Scientific (Osaka, Japan), Ayanda Biosystems (Lausanne, Switzerland), Plexon Inc. (Dallas, TX) / University of North Texas (Denton, TX), and Axion Biosystems (Atlanta, GA).

II.B. Neuronal Cell Culture on MEAs

Dissociated neurons are obtained from embryonic or neonatal stages of animals such as rat or mouse. Various cell culture systems and techniques have been used to study cultured neuronal networks with MEAs: E18 (embryonic day 18) rat hippocampal neurons,[15,22–27] E14-15 mouse spinal cord or cortical neurons,[10,28,29] E17-18 rat cortical neurons,[13,16,30–32] P0-P3 (postnatal day 0 to day 3) rat cortical neurons,[14,33–36] P3 rat hippocampal neurons,[37] and embryonic stem cell derived neurons.[38,39]

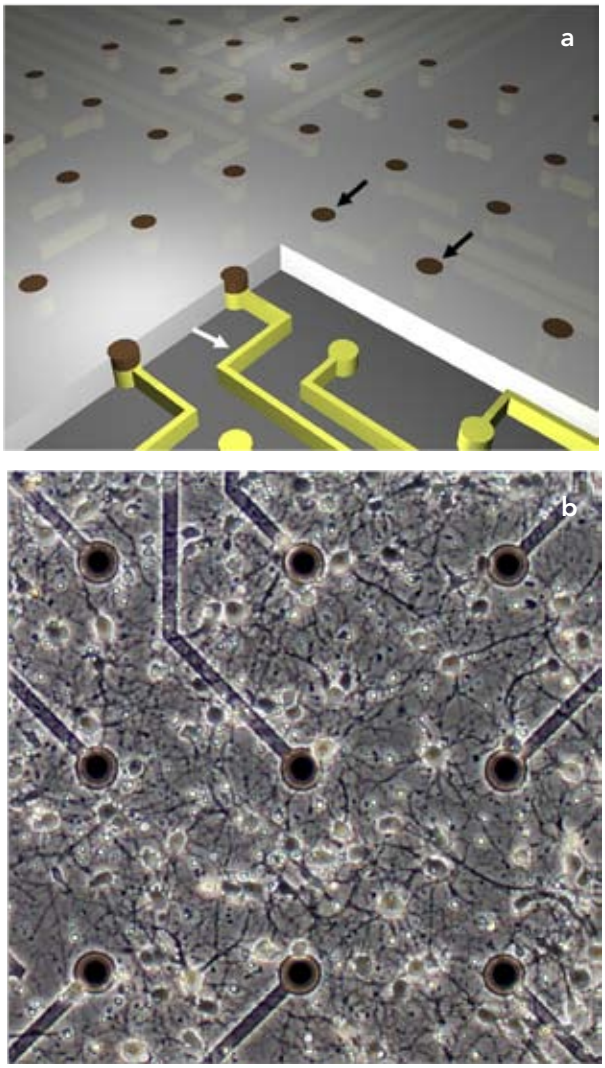

FIGURE 1. (a) Planar-type MEA with an array of embedded microelectrodes (black arrows). Conductor lines (white arrow) are insulated by organic or inorganic materials. (b) Dissociated hippocampal neurons are grown on an MEA. Black dots are electrodes and straight lines are conductor lines. Interelectrode spacing: 200 μm.

In many cases, the cultures were grown under high density (over 1000 cells/mm^2) serum containing conditions. This induces overgrowth of glial cells in the culture, which keeps the culture healthy for the long-term cultures. Instead of serum-containing culture medium, glia-conditioned medium[25,32] or serum-free culture conditions[22,24,40,41] have also been used.

To culture neurons on MEAs, it is necessary to coat the surface with one or another substances that enhances cell attachment and growth. Common coating substances include collagen, polylysine, or laminin, which were adopted from conventional neurobiology experiments. Polyethyleneimine, a synthetic basic polymer, has also been used to achieve longer and stable neuronal growth for long-term cultures.[32] A combination of two molecules is used to improve cell adhesion: polylyine/laminin[29] plus polyetheleneimine/laminin[42] or polyornithine plus Matrigel.[37] In most cases, these molecules are immobilized on the MEA surface without any chemical linkers.

II.C. Neuron-Electrode Coupling of an MEA

As shown in Fig. 2, when cultured neurons are directly grown on top of a microelectrode a unique configuration is formed between the cultured neurons and MEA electrodes. While electrodes are originally used for sensing neural signals, they become a part of the extracellular environment for neuronal growth and development. As neurons are cultured for a few days to weeks on the MEA, long-term culture conditions can influence the performance of the chip. Perhaps most obvious is the continuing development and growth of the neural somata, including movement[43] toward more conducive surfaces, extension on those surfaces including tight coupling to rough and adhesive surfaces, and the extension of axons. The proliferation of supporting astroglia in most culture systems can insulate neurons from electrodes (glial growth beneath the neurons) or tightly couple them (glial growth over the neurons and electrodes).[44] The continuous deposition of protein from media and from neurons is present,[45] fouling the electrodes. Even the insulation can deteriorate over time, as occurs with

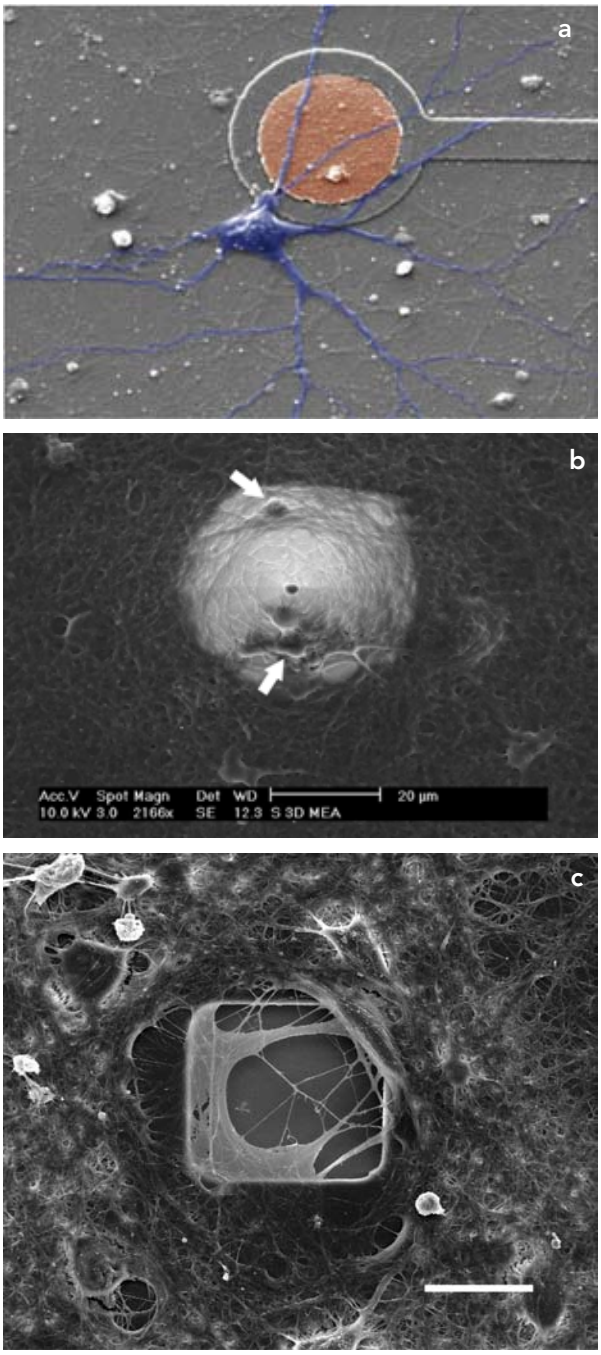

FIGURE 2. Neuron-electrode couplings of various MEAs. (a) Flat type MEA, 11 DIV. (b) 3D tip shape MEA, 24 DIV. Arrows indicate attached somata on the electrode. (c) Recessed type MEA, 24 DIV, scale bar 20 µm. Scanning electron micrograph.

the slow dissolution of oxide and nitride coatings.

Electrodes detect signals originating from extracellular ionic current flow during the generation of action potentials. Although the conductivity of the medium is relatively high, local conductance following the ionic current path can be low enough to generate measurable localized electrical potential changes in the range of tens or hundreds of microvolts. The time course of the signals is as fast as that of the transmembrane action potentials and they reflect on the neuronal activity of the neurons coupled with the electrode.

II.D. Theoretical Modeling of Neural Recordings from Neuron-on-Electrode Configuration

The conventional extracellular recording principle is based on extracellular field theory.[46] A microelectrode about the size of the cell (~10–20 μm in diameter) positioned near the active neurons detects electric potential changes in a conductive extracellular field generated by current flow. The current originates from one part of the cell (usually the axon hillock or soma), which generates an action potential that spreads over other parts (passive dendrites). A membrane current that generates the current flow consists of both capacitive and resistive components (Eq. 1):

$$J_m = J_{cap} + J_{res} = C_m\left(dV_m/dt\right) + G_m V_m \quad (1)$$

where V_m is the transmembrane potential, C_m is the membrane capacitance, and G_m is the membrane conductance.

Extracellular field potentials can be calculated using a distributed current dipole model whose sink is concentrated in axon hillock (or soma) and sources are distributed over dendrites. The polarity of the recorded field potential (spike) strongly depends on the location of the electrode with respect to the spatial distribution of sources and sinks. The extracellular potential at a particular point P can be calculated as follows:

$$V_e(P) = \frac{1}{4\pi\sigma}\sum_i \frac{J_i}{r_i}\Delta S_i \quad (2)$$

where σ is the conductivity of extracellular medium, J_i is the current density over the i^{th} segment (positive for source, negative for sink), r_i is the distance from the i^{th} segment to point P, and ΔS_i is the surface area of the i^{th} segment.[46] A compartmental neuron model based on the Hodgkin-Huxley membrane model is often used, wherein the current density (J_i in Eq. 2) is assumed uniform over the entire surface of the membrane for each compartment and the contributions to the extracellular field potential from each compartment are summed.[47] The compartments may comprise the soma, the axon hillock, and segments of both axons and dendrites, depending on the complexity of the model.

Spike shape is influenced by both cell geometry and cell size. Spike shape can vary depending on the structure of dendritic trees even under the simple assumption of passive dendrites.[48] The cell size determines the cell's input impedance, which in turn affects the magnitude of the membrane currents during depolarization. For a given change of transmembrane potential, large cells can induce membrane currents ($I_m = \Delta V_m / Z_{in}$, where ΔV_m is the transmembrane potential and Z_{in} is the neuron's input impedance) that are larger than for small cells.[46] An alternative way to think of the issue is that larger cells have greater capacitance and hence greater current must flow to discharge and then recharge the membrane. Larger membrane currents imply stronger field potentials based on Eq. 2 ($V_e \propto J_i$).

Axons, which are very small in diameter (e.g., 1 μm), have limited surface area, greater local impedance, much smaller currents, and smaller extracellular potentials. However, the source and sink currents from propagating action potentials are proportional to the second derivative of the action potential signal, a characteristic of the traveling wave.[49] In cultured neural networks, somatic spikes are most readily recorded, with limited recording of axonal spikes.

According to the in vivo recording experiments, somatic spikes can be either positive-negative spikes for pyramidal cells or negative-positive spikes for stellate cells, while axon spikes are biphasic or triphasic depending on whether all phases of the signal are of sufficient amplitude to be recordable.[46] Moreover, somatic spikes (0.7–1.0 ms) are usually

wider than axon spikes (0.4–0.5 ms).[46] An early report on signals recorded with micromachined neural probes provides a graphic explanation of how waveforms are of different polarity depending on the relative position of electrode versus the cell source and sink in vivo.[50] For an electrode quite close to the rapidly depolarizing and large soma, a negative spike is expected, followed by a rebound when the soma acts as a source for other and later depolarizing elements. In the study of extracellular recording from cultured neurons using a glass micropipette, it was reported that somatic spikes were either positive or negative depending on the excitability of the nearby membrane.[51] Axon spikes were mostly negative biphasic spikes, and positive biphasic spikes were recorded from passive dendrites.

In MEA recordings, the size of the recorded action potential can be increased greatly if the electrode and neuron are tightly coupled. Ideally, this is similar to the patch clamp wherein the pipette electrode is completely covered by and seals to the neuron with a leakage resistance to the bathing solution on the order of GΩs. Perhaps the first report of a surface MEA sealing to a neuron was that of Regehr et al., who recorded from a large invertebrate cell sitting on top of the electrode, with a large resulting signal (~0.2–0.3 mV).[52] Fromherz's group used a similar concept to model their recorded signals from a field-effect transistor (FET) array.[53,54] They first observed that the membrane and transistor gate could form an electrical capacitor divider, permitting them to record positive-going signals in the 10 mV range.[53] More sophisticated models, including voltage-gated ion channels, hypothesized that the polarity of recorded cell responses (negative versus positive leading) depended on the local ionic currents in the region of cell adhesion.[55–57] Buitenweg et al. recorded positive somatic spikes from DRG neurons and applied a finite-element modeling technique to study the origin of the amplitude and shape of the extracellular recordings of MEAs.[58] They were able to explain the experimental data by the voltage-sensitive sodium and potassium channel distribution of the lower membrane. Table 1 summarizes some results in the literature describing the observation and modeling of neural recordings from MEAs.

Action potential amplitude can be influenced by the surrounding structure. Recently, recordings of action potentials within microtunnels have been made. The tunnels are 3 μm × 10 μm × 500 μm and have resistances in the tens of MΩs. Even the small currents from axons resulted in large (hundreds of μV) signals within the tunnels.[59]

II.E. An Empirical Study of Spike Shapes Recorded with an MEA

In our work we find that detected waveforms can be categorized by the polarity of the largest peak—positive or negative—and further subdivided into three groups—monophasic, biphasic, or triphasic waveforms (Fig. 3). Negative biphasic spikes have a large negative peak followed by a small positive peak. Negative triphasic spikes have a small positive peak followed by a large negative peak and a small positive peak. Positive triphasic spikes have a large positive peak followed by a comparable or slightly smaller negative peak and a small positive peak.

In experiments done over multiple arrays and cultures, we analyzed the statistics of 60 representative spike waveforms pooled from 175 channels (Fig. 3).[60] The majority of these spike waveforms were negative spikes (80%), while the remainder (20%) were positive. In each category, three subgroups were almost equally distributed. Figure 4 shows distinct neural waveforms from 19 units, each presumably from a unique neuron, as identified using a statistical pattern-clustering algorithm. Most were negative spikes, as were all of the occasional and unusually large waveforms (peak value larger than 200 μV). Three of them were monophasic and two were biphasic. There was one positive biphasic spike close to 200 μV (Fig. 4).

Unfortunately it is not easy to use the spike shape and size to answer the obvious question: from which part of the neuron does the recording come (e.g., axon, hillock, dendritic tree, soma)? The predominance of negative spike waveforms most likely implies that many electrodes are closely coupled to excitable somata and are reporting the

TABLE 1. Observation and modeling of neural recordings from MEAs

Ref.	Observation / Simulation / Action potential (AP) measurement
Regehr et al.[52]	Good signal-to-noise ratio from sealed electrodes, seal resistance essential to record $V_{out} = R_{seal} \times (i_c + i_{ionic})$, $i_c = C_m (dV_m/dt)$ if action potential is fast, $i_c >> i_{ionic}$, waveform similar to 1st derivative if action potential is slow, $i_c \sim i_{ionic}$, various waveforms can appear AP measurement: Intra-, MEA, extra- glass pipette recording
Schätzthauer et al.[56]	Negative spikes recorded when axon stump (leech neuron) was across the electrode High conductance (μ^K and $\mu^{Na} > 1$, $g = \mu g_0$) of attached membrane results in negative leading spikes AP measurement: Intra-, FET array recording
Vassanelli et al.[57] Buitenweg et al.[58]	Positive monophasic spikes from rat neurons Partial depletion or accumulation of ion channels results in positive or negative spikes Na^+ depletion → positive spikes Na^+ accumulation → negative spikes AP measurement: Intra-, FET array, MEA recording

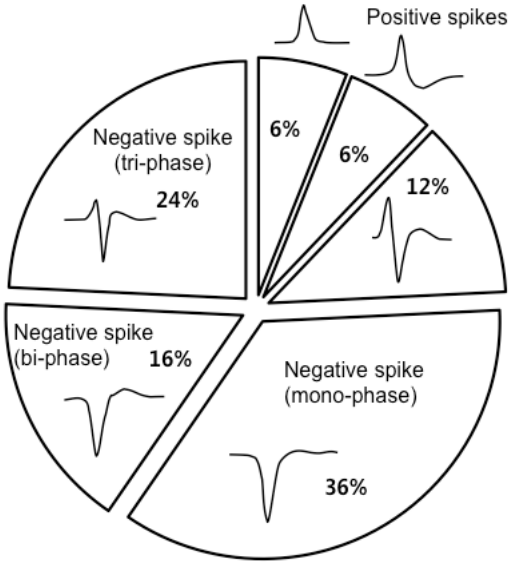

FIGURE 3. Categorized spike waveforms detected by flat type MEAs (n = 60 spikes).[60]

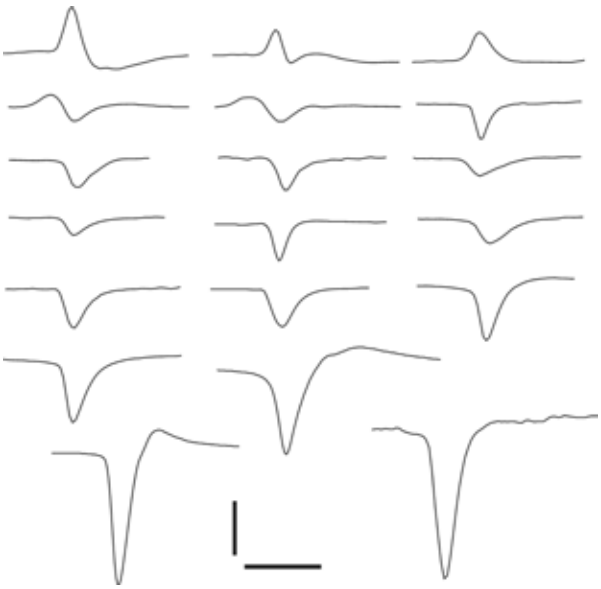

FIGURE 4. Well-isolated 19-spike units after spike sorting. Unusually large spikes are all negative spikes. Scale bar: 200 μV, 1 ms.[60]

TABLE 2. Spike waveforms detected by different geometry of electrodes[23]

%	Positive	Negative	Biphasic [d)]	No. electrodes (No. cultures)
Protruded[a]	56	33	11	153(7)
Recessed[b]	0	100	0	33 (2)
Flat[c]	16	79	5	38 (5)

40 μm protruded, Pt electrode (3D tip shape, 40 μm × 40 μm)
5 μm recessed from the surface , ITO electrode (40 μm × 40 μm)
0.5 μm recessed from the surface, TiN electrode (10 or 30 μm in diameter)
Waveforms with comparable positive and negative peak values

rapid dynamic of the action potential. The limited number of biphasic and triphasic signals suggests that coupling is usually insufficient to detect when the soma acts as a source to action potentials propagating along axons or back into the dendritic tree. If there were much smaller and multiphasic signals, then there would be greater confidence that axonal action potentials were being recorded. The occasional positive-going spikes are more difficult to interpret, as they could be due to excellent sealing to membrane that is acting as a source to other events.

II.F. An Empirical Study of the Effects of Electrode Geometry

The geometry of the electrode can affect the outcome of the recording due to different neuron-electrode interactions or coupling. Table 2 summarizes the portions of spike waveforms (negative spike, positive spike, or other shapes) detected by three different types of MEAs—flat electrode with thin insulator, recessed electrode with thick insulator, and protruded 3D tip electrode with larger surface area.[23] A large portion of the electrodes from flat-type MEAs detected negative spikes. MEAs with recessed electrodes detected only negative spikes. In case of 3D tip type MEAs, there were more electrodes that detected positive spikes than negative or biphasic shapes. It is interesting that we observed rare spike shapes with a positive leading peak followed by a comparable negative peak more frequently in 3D tip MEAs.

Cell-electrode coupling or adhesion can explain the different outcomes related to the electrode geometry. Microscopy studies showed that neurons grew directly on the 3D tip shaped electrode surface and their processes wound around the electrode (Figure 2[b]). In the case of recessed electrodes, the electrodes were located at the bottom of wells that were formed by the thick insulation layer. Scanning electron microscopy preparations suggested that neurons did not grow toward the bottom of the well, leaving electrodes not in contact with cells (Figure 2[c]). In the case of 3D-tip MEAs, the larger fraction of active electrodes detecting positive spikes suggested that passive dendrite components could also be recorded by protruded spikes.

A further conclusion is that flat and recessed electrodes rarely achieve the tight physical coupling necessary to detect the more subtle changes in the source and sink behavior of various components of the neuron. Conversely, the growing interest in nanotextured surfaces (see below) promises to make common both a higher yield of low-amplitude signals as well as signals with a richer repertoire of shapes.

II.G. Changes in Spike Waveform with Maturation

Spike waveforms change as neurons mature. When recordings were made from the same cultures and electrodes, the amplitude and the width of spikes changed with time as the culture matured over a period of several weeks. Figures 5(a) and 5(b) show two examples of spike waveforms that had a monotonic increase during the third week. Peak values

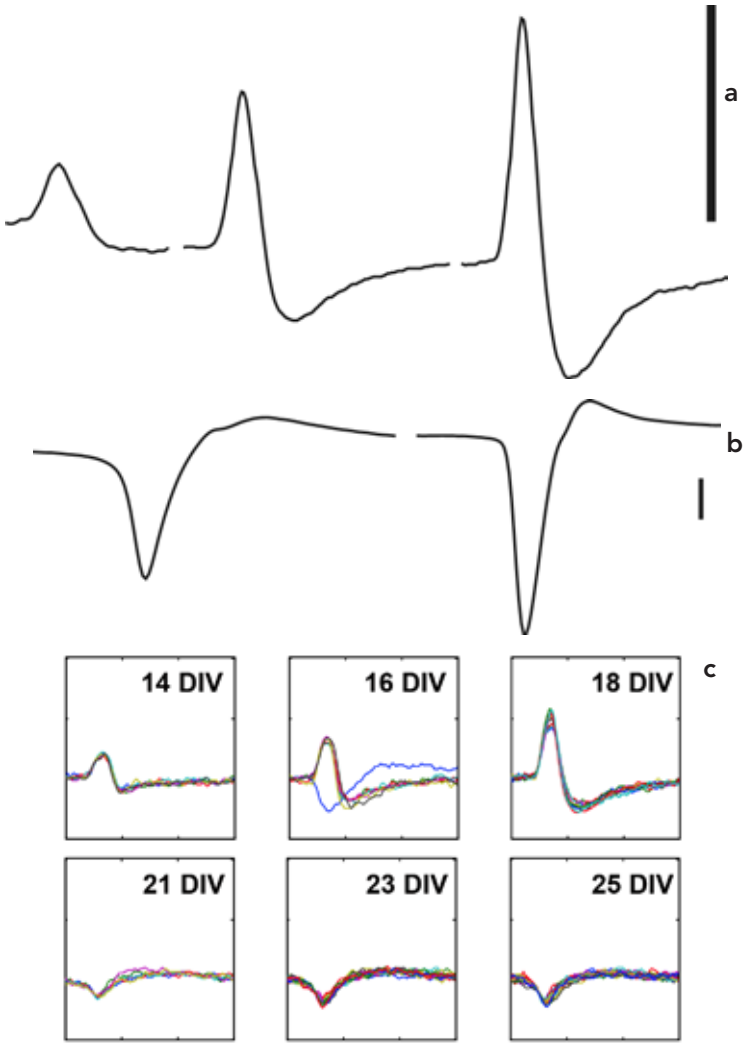

FIGURE 5. Tracking the spike waveform changes as cultures age.[60] (a) Average spike waveform recorded from a similar protruded electrode (16, 18 21 DIV) and (b) a similar flat electrode (14, 24 DIV). Scale bar: 100 μV; each waveform is 3 ms long. (c) Example of abrupt spike waveform changes from positive spikes to negative spikes after 3 weeks in culture. Spikes detected from a similar protruded electrode (*x* axis: 3 ms; *y* axis: 300 μV).

increased and the shape changed from monophasic to a biphasic form. Here it is likely that the successive recordings came from the same neurons. More abrupt changes can also occur during a long-term culture period. Figure 5(c) shows the case when the spike waveform completely changed from a positive spike to a negative spike. It is possible that a cell that was initially coupled with the electrode died, migrated, or became silent, only to be replaced by a different and newly active cell.

The changes in amplitude and width of action potentials with culture age are likely to be associated with the strength and the time course of membrane currents. Two possible explanations are as follows: First, the maturation of sodium and potassium channels that are associated with the generation of an action potential could have modulated the spike waveforms. Comparative studies of immature and

mature brain tissues show that there are increases in membrane conductance and current density due to the maturation of ion channels.[61,62] This reported change of the time course of the current density can change the shape of spikes. Second, the development of the cell geometry, such as the complexity of dendritic trees or the size of soma, could lead to the change of shapes. More dendrites near electrodes would have increased the current density that may have contributed to the strength of the extracellular field potential.

II.H. Biological Factors in the Outcome of Neural Recordings

In many cases, signals are not recorded due to poor or insufficient coupling. Our study of the relationship between the cell-electrode coupling and the yield of signal detection suggests that the signal recordings were possible only when neurons were in direct contact with the electrode.[63] When neurons were further than a few tens of micrometers in distance, it was not possible to detect any signals. It was notable that some electrodes did not detect any signal despite the presence of cells on top of the electrode, which implies that there are other biological factors that play an important role in the outcome of the recordings.

One major source of change in action potential shape is that, initially and for the first week or more, neurons may not be conditioned or developed properly to generate action potentials. There is a maturation period for dissociated neurons to obtain membrane excitability (ion channel expression, ion channel density, cell size, cell geometry, synapse formation, etc.). It takes even longer for neurons to receive synaptic inputs from other neurons and form coordinated network activity.[64–66] Synaptogenesis also occurs in the early stage of the culture and takes some time for full expression.[1] Therefore, it is likely that some of the visibly coupled neurons may belong to the immature group.

The extracelluar environment is also modulated during this time, with potential effects on spike shapes. The most noticeable cells are glial cells such as astrocytes, which are abundant in most of the neuronal cultures, even in serum-free conditions.[67,68] When glial cells are present, they usually form a layer and can locate underneath or on top of the neuron of interest. If they happen to locate between the neuron and an electrode surface, they might interfere with the signal transmission, which has been speculated to be the cause of silent neural electrodes that were chronically implanted for months.[69] On the other hand, if the glial layer can be on top of the neurons such that they form a glial blanket, this can enhance the signal strength by confining the extracellular current flow path and increasing the effective local resistance. We have one report showing that glia proliferate both under and over neural processes in culture.[44] Other than the physical roles, astrocytes certainly affect neurons metabolically and by modulating synaptic transmission.[67,70]

III. ENGINEERING IN VITRO NEURAL INTERFACES

III.A. MEA Electrode Modification by Nanomaterials

Decreasing the electrode-electrolyte interfacial impedance is essential to achieve high-quality neural recordings. With lower impedance values, less background noise and higher stimulation efficiency are achievable. A low-impedance MEA has been obtained by several methods: electroplating platinum black[71–74] or gold colloids,[75] three-dimensional electrode structure,[76] or TiN sputtering.[77]

Recently, nanostructures or carbon nanotubes (CNTs) have been used to modify the electrode, and showed some promising results. These nanomaterials provide higher electrode surface area that is electrochemically active for neural recording or electrical stimulation. Kim et al. used a flake gold nanostructure to achieve large surface area and mechanically stable structures on the electrode surface.[78] Park et al. reported electroplated 3D-nanoporous Pt microelectrodes that showed higher mechanical strength than conventional platinum black microelectrodes.[79] Gabay et al. used CNTs to fabricate mesh-like electrode surfaces, which resulted in extremely low electrode impedances and large signals.[80] Keefer et al. plated CNT material

on an electrode and showed decreased impedances.[81] One can expect even more materials to emerge from the nanotechnology field that will improve neural interface design.

It is also noticeable that neurons had a strong adhesive response to natural CNT mesh-like electrodes, and the recorded signals were close to 1 mV, which was a few orders of magnitude larger than from conventional microelectrodes.[80] Thus, the nanomaterials could have an influence on cell-electrode coupling due to mechanobiological interactions between the electrode and cell membrane.

III.B. Electrode Modification Using Self-Assembled Monolayers

MEA electrodes can be modified through chemical surface modification methods. The main purpose of these methods is to convert the electrode surfaces into biologically active or functional sites, so that the interaction between neurons and electrodes can be controllable to a certain degree. In this approach, the key technology is to utilize self-assembled monolayers (SAMs) with special functional groups (e.g., amine, thiol, carboxyl) to immobilize biomolecules through covalent linking schemes.

Two common SAMs are alkanethiol SAMs and organosilane SAMs. The former is specific to gold surfaces and the latter is applicable to glassy surfaces with hydroxyl groups. Our recent study suggests that a SAM-based covalent linking scheme for the surface modification of MEA insulators can also modify the electrode surfaces.[41] Low-impedance TiN MEA (30 μm in diameter) was reacted with an organosilane ([3-glycidoxypropyl] trimethoxysilane, 3GPS) and polylysine was linked through the covalent bond formed between the epoxide group of 3GPS and the amine group of polylysine. A high-quality neural recording and stimulation was possible from the cultured hippocampal neuronal networks. Despite the successful experiments, it was noticeable that the 3GPS modification increased the electrode impedance by a factor of 2.8, which is attributed to the addition of an adlayer (3GPS SAM) on the bare electrode surface. However, the increase was modest in the sense that the impedance of the modified electrodes was less than 150 kΩ at 1 kHz and the measured background noise level was sufficiently small (2.1–2.9 μVrms) to obtain high SNR neural recordings for a few weeks (SNR: 4.5 to 15.8).

Figure 6 shows an example of noise level, electrode impedance, and neural recordings from SAM-treated MEAs. In this example, three SAMs (3GPS, 11-mercaptoundecanoic acid [11-MUA], 3-amonipropyltrimethoxysilane [3APS]) that were used in the literature for immobilizing biomolecules were used to modify MEAs with titanium nitride (3GPS TiN, 3APS TiN), platinum black (3APS Pt), and electroplated gold (11-MUA Au). For TiN electrodes, the modified electrode impedance was lower than other electrodes due to their initial low values (Figure 6[a]). Au and Pt electrodes had relatively high impedance and noise level, but it was possible to obtain some high-SNR recordings from cultured neurons through the electrodes (Figure 6[b]).

III.C. MEA Surface Engineering

Surface patterned MEAs have been introduced to control the cultured neurons for two purposes: (1) to control the adhesion and growth of the neurons to construct and study ordered neuronal networks and (2) to localize neurons to increase the yield of cell-electrode coupling. For these purposes, several surface patterning approaches have been reported.

Chemical patterning methods use surface microprinting techniques and chemical linking schemes to pattern and immobilize biomolecules. Two popular micropatterning techniques are photoresist-based patterning and microcontact printing. The photoresist-based patterning utilizes the lift-off process of conventional photolithography. Using this process, cell-adhesive biomolecules such as polylysine were patterned on MEAs.[24,82,83] Microcontact printing uses a silicone rubber stamp with a defined micropattern generated by soft lithography. This technique provides a simple and easy way of printing biomolecules on MEA surfaces.[40,41,84,85] In addition to micropatterning techniques, SAM-based MEA surface modification schemes have been reported to control the immobilization of biomolecules on the MEA insulator surfaces. 3GPS has been shown to be effective

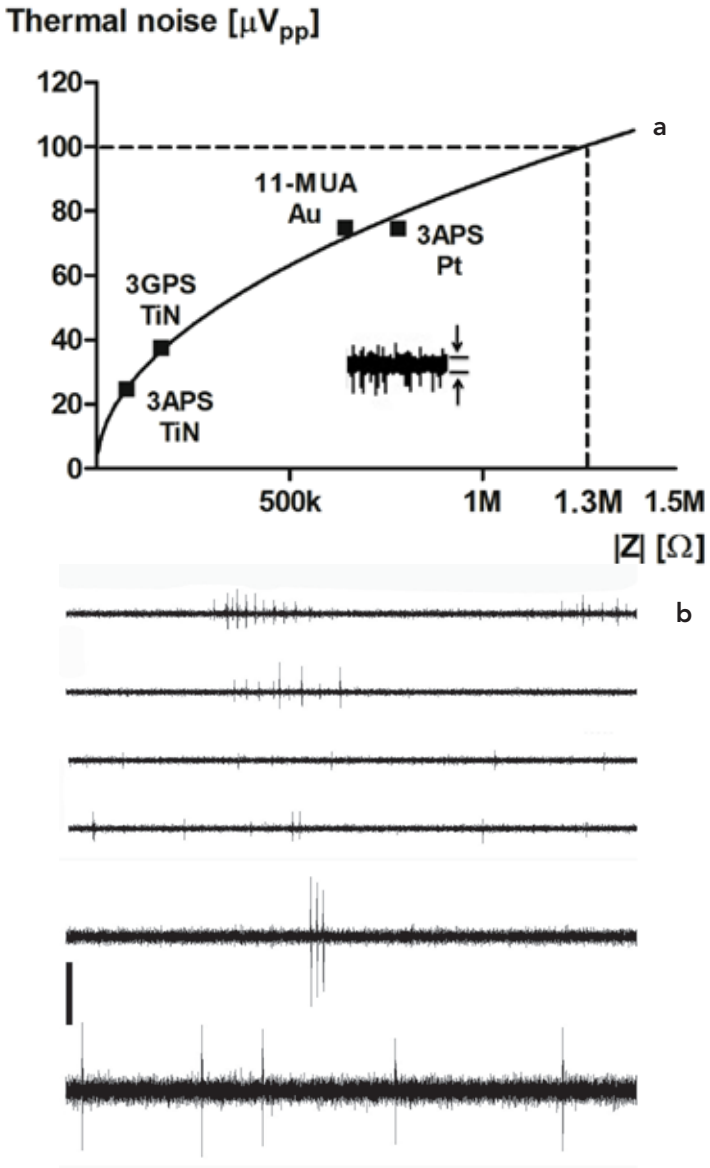

FIGURE 6. (a) Theoretical thermal noise peak-to-peak value curve and measured values (square dots) from SAM modified electrodes. Z value at 1 kHz. (b) Examples of neural recording from 3APS modified platinum black electrodes (top two traces, 33 DIV, SNR 6.5, 8.8), 3APS modified titanium nitride electrodes (middle two traces, 19 DIV, SNR 5.7, 7,5), and 11-MUA modified gold electrodes (bottom two traces, 15 DIV, SNR 18.8, 8.0). Time span: 2 s; scale bar: 100 μV.[60]

for silicon dioxide–, nitride-, and polyimide-based MEA surfaces.[41] Polylysine patterns and cultured neurons were successfully implemented on three different types of MEA surfaces. To utilize alkanethiol chemistry, gold-coated MEAs were developed and 11-mercaptoundecanoic acid (11-MUA) was used to immobilize and pattern polylysine and polyethylene glycol.[84]

Physical patterning methods involve the fabrication of microstructures on MEAs to control the adhesion and growth of neurons with respect to the electrodes. A few materials that were used

for microstructures were polyimide,[71] SU-8,[86] agarose hydrogel,[25,87] or polydimethoxysiloxane (PDMS).[59,88,89] A network of microgrooves made of polyimide (10 μm in thickness) was constructed on MEAs to grow cortical neurons into patterned networks.[71] A similar approach was used to topologically guide snail neurons on FET arrays using SU-8 (15 μm).[86] Micro-picket fences were made of polyimide to immobilize neurons on top of the recording electrode (transistor type).[90] MEAs with agarose hydrogel structures have been reported with different fabrication methods. Suzuki et al. used a photothermal etching technique to make microchambers on electrodes and tunnel-shaped channels that connected the microchambers while cultivating neurons.[25] An in situ stepwise pattern modification technique allowed them to construct neuronal networks with controlled polarity. Kang et al. used the MIMIC (micro-molding in capillary) technique to produce an agarose hydrogel microarray for a novel cell-based biosensing platform based on MEAs.[87] In both works, the cell-repulsive property of agarose hydrogel facilitated the confinement of neurons on microelectrodes. Closed PDMS microchannel devices were attached to an MEA to confine and guide neuronal growth.[88,91] Using this technique, Claverol-Tinture et al. showed the recording of propagating action potentials from a single neuron.[89,92] The surface of the MEAs was physically divided by a compartmentalized PDMS device that enabled the study of signal transduction in neurons.[59,93] Separate recordings from somal and axonal compartments were demonstrated from the platform.[59] While PDMS devices are a promising platform for high-throughput cell biology, novel MEA platforms are yet to come in this field.

III.D. Beyond Extracellular Recording Limits

Extracellular recordings by metal electrodes can detect only action potentials, while intracellular or whole-cell patch recording can record subthreshold synaptic activity as well as suprathreshold activity (action potentials). Although extracellular recordings provide long-term noninvasive neural interfaces, the lack of subthreshold activity can limit the analysis of neural information processing in the network.

It has been suggested by a few groups that it would be possible to record signals resembling transmembrane potentials with extracellular electrodes by adjusting a seal resistance between neuron and electrode.[52,94,95] With a high seal resistance, capacitive coupling can be obtained and the recorded signal would be a miniaturized version of transmembrane potential.

Recently, the Spira group has reported "in-cell recordings" by extracellular neural interfaces through a biomimetic approach.[96] They designed an electrode with protruding gold spines that imitate dendritic spines in structure, and functionalized the surface with arginine–glycine–aspartic acid (RGD) peptides. The structure of the gold spines and the surface peptides induced the engulfing of the spine by plasma membrane, which formed a high density of ionic channels tightly interfaced with the electrode surface. With these electrodes, they were able to record subthreshold synaptic potential as well as action potentials. The action-potential waveforms were very similar to those recorded by an intracellular glass electrode, and the amplitudes were as large as 25 mV.

CONCLUSIONS AND SUMMARY

Cell-electrode coupling and electrode interface are important in that they have an influence on the yield of MEA recordings and spike waveforms. In addition, biological factors also play a pivotal role in overall MEA system performance. Neural interface issues related to signal recordings can also be extended to investigate and explore neural engineering problems in brain-machine-interface applications.

REFERENCES

1. Valor LM, Charlesworth P, Humphreys L, Anderson CN, Grant SG. Network activity-independent coordinated gene expression program for synapse assembly. Proc Natl Acad Sci U S A. 2007;104(11):4658–63.
2. Dotti CG, Sullivan CA, Banker GA. The establishment of polarity by hippocampal neurons in culture. J Neurosci. 1988;8(4):1454–68.
3. Taylor AM, Blurton-Jones M, Rhee SW, Cribbs

DH, Cotman CW, Jeon NL. A microfluidic culture platform for CNS axonal injury, regeneration and transport. Nat Methods. 2005;2(8):599–605.
4. Bi GQ, Poo MM. Synaptic modifications in cultured hippocampal neurons: dependence on spike timing, synaptic strength, and postsynaptic cell type. J Neurosci. 1998;18(24):10464–72.
5. Bi G, Poo M. Distributed synaptic modification in neural networks induced by patterned stimulation. Nature. 1999;401(6755):792–6.
6. Campenot RB, Lund K, Mok SA. Production of compartmented cultures of rat sympathetic neurons. Nat Protoc. 2009;4(12):1869–87.
7. Segal MM, Furshpan EJ. Epileptiform activity in microcultures containing small numbers of hippocampal neurons. J Neurophysiol. 1990;64(5):1390–9.
8. Kleinfeld D, Kahler KH, Hockberger PE. Controlled outgrowth of dissociated neurons on patterned substrates. J Neurosci. 1988;8(11):4098–120.
9. Gahwiler BH, Capogna M, Debanne D, McKinney RA, Thompson SM. Organotypic slice cultures: a technique has come of age. Trends Neurosci. 1997;20(10):471–7.
10. Gross GW, Williams AN, Lucas JH. Recording of spontaneous activity with photoetched microelectrode surfaces from mouse spinal neurons in culture. J Neurosci Methods. 1982;5:13–22.
11. Thomas CAJ, Springer PA, Loeb GE, Berwald-Netter Y, Okun LM. A miniature microelectrode array to monitor the bioelectric activity of cultured cells. Exp Cell Res. 1972;74:61–6.
12. Pine J. Recording action potentials from cultured neurons with extracellular microcircuit electrodes. J Neurosci Methods. 1980;2(1):19–31.
13. Jimbo Y, Kawana A, Parodi P, Torre V. The dynamics of a neuronal culture of dissociated cortical neurons of neonatal rats. Biol Cybern. 2000;83:1–20.
14. Eytan D, Marom S. Dynamics and effective topology underlying synchronization in networks of cortical neurons. J Neurosci. 2006;26(33):8465–76.
15. Baruchi I, Volman V, Raichman N, Shein M, Ben-Jacob E. The emergence and properties of mutual synchronization in in vitro coupled cortical networks. Eur J Neurosci. 2008;28(9):1825–35.
16. Wagenaar DA, Madhavan R, Pine J, Potter SM. Controlling bursting in cortical cultures with closed-loop multi-electrode stimulation. J Neurosci. 2005;25(3):680–8.
17. Mathieson K, Cunningham W, Marchal J, Melone J, Horn M, O'Shea V, Smith KM, Litke A, Chichilnisky EJ, Rahman M. Fabricating high-density microarrays for retinal recording. Microelectronic Engineering. 2003;67–68:520–7.
18. Bucher V, Brunner B, Leibrock C, Schubert M, Nisch W. Electrical properties of a light-addressable microelectrode chip with high electrode density for extracellular stimulation and recording of excitable cells. Biosens Bioelectron. 2001 2001;16(3):205–10.
19. Frey U, Egert U, Heer F, Hafizovic S, Hierlemann A. Microelectronic system for high-resolution mapping of extracellular electric fields applied to brain slices. Biosens Bioelectron. 2009;24(7):2191–8.
20. Berdondini L, Imfeld K, Maccione A, Tedesco M, Neukom S, Koudelka-Hep M, Martinoia S. Active pixel sensor array for high spatio-temporal resolution electrophysiological recordings from single cell to large scale neuronal networks. Lab Chip. 2009;9(18):2644–51.
21. Eversmann B, Jenkner M, Hofmann F, Paulus C, Brederlow R, Holzapfl B, Fromherz P, Merz M, Brenner M, Schreiter M, Gabl R, Plehnert K, Steinhauser M, Eckstein G, Schmitt-Landsiedel D, Thewes R. A 128 × 128 CMOS Biosensor Array for Extracellular Recording of Neural Activity. IEEE J Solid-State Circuits. 2003;38(12):2306–17.
22. Jun SB, Hynd MR, Dowell-Mesfin N, Smith KL, Turner JN, Shain W, Kim S J. Low-density neuronal networks cultured using patterned poly-l-lysine on microelectrode arrays. J Neurosci Methods. 2007;160(2):317–26.
23. Nam Y, Wheeler BC, Heuschkel MO. Neural recording and stimulation of dissociated hippocampal cultures using microfabricated three-dimensional tip electrode array. J Neurosci Methods. 2006;155(2):296–9.

24. Chang JC, Brewer GJ, Wheeler BC. Modulation of neural network activity by patterning. Biosens Bioelectron. 2001;16:527–33.
25. Suzuki I, Sugio Y, Jimbo Y, Yasuda K. Stepwise pattern modification of neuronal network in photo-thermally-etched agarose architecture on multi-electrode array chip for individual-cell-based electrophysiological measurement. Lab Chip. 2005;5(3):241–7.
26. Sokal DM, Mason R, Parker TL. Multi-neuronal recordings reveal a differential effect of thapsigargin on bicuculline- or gabazine-induced epileptiform excitability in rat hippocampal neuronal networks. Neuropharmacology. 2000;39(12):2408–17.
27. Golan H, Mikenberg K, Greenberger V, Segal M. GABA withdrawal modifies network activity in cultured hippocampal neurons. Neural Plasticity. 2000;7(1–2):31–42.
28. Selinger JV, Pancrazio JJ, Gross GW. Measuring synchronization in neuronal networks for biosensor applications. Biosens Bioelectron. 2004;19(7):675–83.
29. Morefield SI, Keefer EW, Chapman KD, Gross GW. Drug evaluations using neuronal networks cultured on microelectrode arrays. Biosens Bioelectron. 2000;15(7–8):383–96.
30. Wagenaar DA, Pine J, Potter SM. Searching for plasticity in dissociated cortical cultures on multi-electrode arrays. J Negat Results Biomed. 2006;5:16.
31. Bakkum DJ, Chao ZC, Potter SM. Spatio-temporal electrical stimuli shape behavior of an embodied cortical network in a goal-directed learning task. J Neural Eng. 2008;5(3):310–23.
32. van Pelt J, Wolters PS, Corner MA, Rutten WL, Ramakers GJ. Long-term characterization of firing dynamics of spontaneous bursts in cultured neural networks. IEEE Trans Biomed Eng. 2004;51(11):2051–62.
33. Eytan D, Brenner N, Marom S. Selective adaptation in networks of cortical neurons. J Neurosci. 2003;23(28):9349–56.
34. Eytan D, Minerbi A, Ziv N, Marom S. Dopamine-induced dispersion of correlations between action potentials in networks of cortical neurons. J Neurophysiol. 2004;92(3):1817–24.
35. Shahaf G, Marom S. Learning in networks of cortical neurons. J Neurosci. 2001;21(22):8782–8.
36. Segev R, Shapira Y, Benveniste M, Ben-Jacob E. Observation and modeling of synchronized bursting in two-dimensional neural network. Phys Rev E. 2001;64(011920).
37. Ruaro ME, Bonifazi P, Torre V. Toward the neurocomputer: image processing and pattern recognition with neuronal cultures. IEEE Trans Biomed Eng. 2005;52(3):371–83.
38. Illes S, Theiss S, Hartung HP, Siebler M, Dihne M. Niche-dependent development of functional neuronal networks from embryonic stem cell–derived neural populations. BMC Neurosci. 2009;10:93.
39. Illes S, Fleischer W, Siebler M, Hartung HP, Dihne M. Development and pharmacological modulation of embryonic stem cell-derived neuronal network activity. Exp Neurol. 2007;207(1):171–6.
40. James CD, Spence AJ, Dowell-Mesfin NM, Hussain RJ, Smith KL, Craighead HG, Isaacson MS, Shain W, Turner JN. Extracellular recordings from patterned neuronal networks using planar microelectrode arrays. IEEE Trans Biomed Eng. 2004;51(9):1640–8.
41. Nam Y, Branch DW, Wheeler BC. Epoxy-silane linking of biomolecules is simple and effective for patterning neuronal cultures. Biosens Bioelectron. 2006;22(5):589–97.
42. Potter SM, DeMarse TB. A new approach to neural cell culture for long-term studies. J Neurosci Methods. 2001;110(1–2):17–24.
43. Corey JM, Wheeler BC, Brewer GJ. Compliance of hippocampal neurons to patterned substrate networks. J Neurosci Res. 1991;30:300–7.
44. Nam Y, Wheeler BC, editors. Imaging locations of neurons vs. glia in low density culture. IEEE EMBS Conference on Neural Engineering; 2005; Arlington, VA, USA.
45. Branch DW, Wheeler BC, Brewer GJ, Leckband DE. Long-term stability of grafted polyethylene glycol surfaces for use with microstamped substrates in neuronal cell culture. Biomaterials. 2001;22(10):1035–47.
46. Boulton AA, Baker GB, Vanderwolf CH, Hum-

phrey DR, Schmidt EM. Extracellular single-unit recording methods. Neurophysiological techniques: Humana Press; 1991. p. 1–64.
47. Moffitt MA, McIntyre CC. Model-based analysis of cortical recording with silicon microelectrodes. Clin Neurophysiol. 2005;116(9):2240–50.
48. Rall W. Electrophysiology of a dendritic neuron model. Biophys J. 1962;2(2)Pt 2:145–67.
49. Plonsey R. The active fiber in a volume conductor. IEEE Trans Biomed Eng. 1974;21(5):371–81.
50. Drake KL, Wise KD, Farraye J, Anderson DJ, BeMent SL. Performance of planar multisite microprobes in recording extracellular single-unit intracortical activity. IEEE Trans Biomed Eng. 1988;35(9):719–32.
51. Claverol-Tinture E, Pine J. Extracellular potentials in low-density dissociated neuronal cultures. J Neurosci Methods. 2002;117(1):13–21.
52. Regehr WG, Pine J, Cohan CS, Mischke MD, Tank DW. Sealing cultured invertebrate neurons to embedded dish electrodes facilitates long-term stimulation and recording. J Neurosci Methods. 1989;30:91–106.
53. Fromherz P, Offenhausser A, Vetter T, Weis J. A neuron-silicon junction: a Retzius cell of the leech on an insulated-gate field-effect transistor. Science. 1991;252(5010):1290–3.
54. Fromherz P, Muller CO, Weis R. Neuron transistor: Electrical transfer function measured by the patch-clamp technique. Phys Rev Lett. 1993;71(24):4079–82.
55. Jenkner M, Muller B, Fromherz P. Interfacing a silicon chip to pairs of snail neurons connected by electrical synapses. Biol Cybern. 2001;84(4):239–49.
56. Schatzthauer R, Fromherz P. Neuron-silicon junction with voltage-gated ionic currents. Eur J Neurosci. 1998;10(6):1956–62.
57. Vassanelli S, Fromherz P. Transistor records of excitable neurons from rat brain. Appl Phys A. 1998;66:459–63.
58. Buitenweg JR, Rutten WL, Marani E. Modeled channel distributions explain extracellular recordings from cultured neurons sealed to microelectrodes. IEEE Trans Biomed Eng. 2002c;49(12 Pt 2):1580–90.
59. Dworak BJ, Wheeler BC. Novel MEA platform with PDMS microtunnels enables the detection of action potential propagation from isolated axons in culture. Lab Chip. 2009;9(3):404–10.
60. Nam Y. Engineering Principles to design and analyze patterned neuronal cultures using multielectrode arrays. Urbana: University of Illinois; 2005.
61. Costa PF. The kinetic parameters of sodium currents in maturing acutely isolated rat hippocampal CA1 neurones. Dev Brain Res. 1996;91(1):29–40.
62. Picken Bahrey HL, Moody WJ. Early development of voltage-gated ion currents and firing properties in neurons of the mouse cerebral cortex. J Neurophysiol. 2003;89(4):1761–73.
63. Nam Y, Chang J, Khatami D, Brewer GJ, Wheeler BC. Patterning to enhance activity of cultured neuronal networks. IEE Proc Nanobiotechnol. 2004;151(3):109–15.
64. Brewer GJ, Boehler MD, Pearson RA, DeMaris AA, Ide AN, Wheeler BC. Neuron network activity scales exponentially with synapse density. J Neural Eng. 2009;6(1):014001.
65. Ichikawa M, Muramoto K, Kobayashi K, Kawahara M, Kuroda Y. Formation and maturation of synapses in primary cultures of rat cerebral cortical cells: an electron microscopic study. Neurosci Res. 1993;16(2):95–103.
66. Muramoto K, Ichikawa M, Kawahara M, Kobayashi K, Kuroda Y. Frequency of synchronous oscillations of neuronal activity increases during development and is correlated to the number of synapses in cultured cortical neuron networks. Neurosci Lett. 1993;163(2):163–5.
67. Chang JC, Brewer GJ, Wheeler BC. Neuronal network structuring induces greater neuronal activity through enhanced astroglial development. J Neural Eng. 2006;3(3):217–26.
68. Nam Y, Brewer GJ, Wheeler BC. Development of astroglial cells in patterned neuronal cultures. J Biomater Sci Polym Ed. 2007;18(8):1091–100.
69. Polikov VS, Tresco PA, Reichert WM. Response of brain tissue to chronically implanted neural electrodes. J Neurosci Methods. 2005;148(1):1–18.
70. Boehler MD, Wheeler BC, Brewer GJ. Added astroglia promote greater synapse density and

higher activity in neuronal networks. Neuron Glia Biol. 2007;3:127–40.
71. Jimbo Y, Robinson HPC, Kawana A. Simultaneous measurement of intracellular calcium and electrical activity from patterned neural networks in culture. IEEE Trans Biomed Eng. 1993;40(8):804–10.
72. Novak JL, Wheeler BC. Recording from the *Aplysia* abdominal ganglion with a planar microelectrode array. IEEE Trans Biomed Eng. 1986;33(2):196–202.
73. Borkholder DA, Bao J, Maluf NI, Perl ER, Kovacs GT. Microelectrode arrays for stimulation of neural slice preparations. J Neurosci Methods. 1997;77(1):61–6.
74. Oka H, Shimono K, Ogawa R, Sugihara H, Taketani M. A new planar multielectrode array for extracellular recording: application to hippocampal acute slice. J Neurosci Methods. 1999;93(1):61–7.
75. Gross GW, Wen WY, Lin JW. Transparent indium-tin oxide electrode patterns for extracellular, multisite recording in neuronal cultures. J Neurosci Methods. 1985;15(3):243–52.
76. Heuschkel MO, Fejtl M, Raggenbass M, Bertrand D, Renaud P. A three-dimensional multi-electrode array for multi-site stimulation and recording in acute brain slices. J Neurosci Methods. 2002;114(2):135–48.
77. Egert U, Schlosshauer B, Fennrich S, Nisch W, Fejtl M, Knott T, Haemmerle H. A novel organotypic long-term culture of the rat hippocampus on substrate-integrated multielectrode array. Brain Res Brain Res Protoc. 1998;2:229–42.
78. Kim JH, Kang G, Nam Y, Choi YK. Surface-modified microelectrode array with flake nanostructure for neural recording and stimulation. Nanotechnology. 2010;21(8):85303.
79. Park S, Song YJ, Boo H, Chung TD. Nanoporous Pt microelectrode for neural stimulation and recording: in vitro characterization. J Phys Chem C. 2010;114(19):8721–6.
80. Gabay T, Ben-David M, Kalifa I, Sorkin R, Abrams ZR, Ben-Jacob E, Hanein Y. Electrochemical and biological properties of carbon nanotube based multi-electrode arrays. Nanotechnology. 2007;18(3):035201.
81. Keefer EW, Botterman BR, Romero MI, Rossi AF, Gross GW. Carbon nanotube coating improves neuronal recordings. Nat Nanotechnol. 2008;3(7):434–9.
82. Chang JC, Brewer GJ, Wheeler BC. Microelectrode array recordings of patterned hippocampal neurons for four weeks. Biomed Microdevices. 2000;2(4):245–53.
83. Segev R, Benveniste M, Hulata E, Cohen N, Palevski A, Kapon E, Shapira Y, Ben Jacob E. Long term behavior of lithographically prepared in vitro neuronal networks. Phys Rev Lett. 2002;88(11):118102.
84. Nam Y, Chang JC, Wheeler BC, Brewer GJ. Gold-coated microelectrode array with thiol linked self-assembled monolayers for engineering neuronal cultures. IEEE Trans Biomed Eng. 2004;51(1):158–65.
85. Jungblut M, Knoll W, Thielemann C, Pottek M. Triangular neuronal networks on microelectrode arrays: an approach to improve the properties of low-density networks for extracellular recording. Biomed Microdevices. 2009;11(6):1269–78.
86. Merz M, Fromherz P. Polyester microstructures for topographical control of outgrowth and synapse formation of snail neurons. Adv Mater. 2002;14(2):141–4.
87. Kang G, Lee JH, Lee CS, Nam Y. Agarose microwell based neuronal micro-circuit arrays on microelectrode arrays for high throughput drug testing. Lab Chip. 2009;9(22):3236–42.
88. Morin F, Nishimura N, Griscom L, Lepioufle B, Fujita H, Takamura Y, Tamiya E. Constraining the connectivity of neuronal networks cultured on microelectrode arrays with microfluidic techniques: a step towards neuron-based functional chips. Biosens Bioelectron. 2006;21(7):1093–100.
89. Claverol-Tinture E, Cabestany J, Rosell X. Multisite recording of extracellular potentials produced by microchannel-confined neurons in-vitro. IEEE Trans Biomed Eng. 2007;54(2):331–5.
90. Zeck G, Fromherz P. Noninvasive neuroelectronic interfacing with synaptically connected snail neurons immobilized on a semiconductor chip. Proc

Natl Acad Sci U S A. 2001;98(18):10457–62.
91. Griscom L, Degenaar P, LePioufle B, Tamiya E, Fujita H. Techniques for patterning and guidance of primary culture neurons on microelectrode arrays. Sensors Actuators B-Chem. 2002;83(1–3):15–21.
92. Claverol-Tinture E, Ghirardi M, Fiumara F, Rosell X, Cabestany J. Multielectrode arrays with elastomeric microstructured overlays for extracellular recordings from patterned neurons. J Neural Eng. 2005;2(2):L1–7.
93. Ravula SK, McClain MA, Wang MS, Glass JD, Frazier AB. A multielectrode microcompartment culture platform for studying signal transduction in the nervous system. Lab Chip. 2006;6(12):1530–6.
94. Grattarola M, Martinoia S. Modeling the neuron-microtransducer junction: from extracellular to patch recording. IEEE Trans Biomed Eng. 1993;40(1):35–41.
95. Jenkner M, Fromherz P. Bistability of membrane conductance in cell adhesion observed in a neuron transistor. Phys Rev Lett. 1997;79:4705–8.
96. Hai A, Shappir J, Spira ME. In-cell recordings by extracellular microelectrodes. Nat Methods. 2010;7(3):200–2.